Chapter 12

A Novel Quantitative Method for the Detection of Lipofuscin, the Main By-Product of Cellular Senescence, in Fluids

Sophia V. Rizou, Konstantinos Evangelou, Vassilios Myrianthopoulos, Iordanis Mourouzis, Sophia Havaki, Aikaterini Athanasiou, Panagiotis V. S. Vasileiou, Aggelos Margetis, Athanassios Kotsinas, Nikolaos G. Kastrinakis, Petros Sfikakis, Paul Townsend, Emmanuel Mikros, Constantinos Pantos, and Vassilis G. Gorgoulis

Abstract

Lipofuscin accumulation is a hallmark of senescence. This nondegradable material aggregates in the cytoplasm of stressed or damaged cells due to metabolic imbalance associated with aging and age-related diseases. Indications of a soluble state of lipofuscin have also been provided, rendering the perspective of monitoring such processes via lipofuscin quantification in liquids intriguing. Therefore, the development of an accurate and reliable method is of paramount importance. Currently available assays are characterized by inherent pitfalls which demote their credibility. We herein describe a simple, highly specific and sensitive protocol for measuring lipofuscin levels in any type of liquid. The current method represents an evolution of a previously described assay, developed for in vitro and in vivo senescent cell recognition that exploits a newly synthesized Sudan Black-B analog (GL13). Analysis of human clinical samples with the modified protocol provided strong evidence of its usefulness for the exposure and surveillance of age-related conditions.

Key words Lipofuscin, GL13 (SenTraGor™), Senescence, Biological fluids, Aging, Age-related diseases

1 Introduction

We have recently shown that cytoplasmic lipofuscin aggregation is a landmark of senescence [1, 2]. The latter represents a cellular response mechanism against stress or damage [3–7]. Subsequently, we developed a novel reagent (GL13) and a hybrid histochemical–immunohistochemical method that allows for recognition of

Sophia V. Rizou, Konstantinos Evangelou, Vassilios Myrianthopoulos, and Iordanis Mourouzis contributed equally to this work.

Marco Demaria (ed.), *Cellular Senescence: Methods and Protocols*, Methods in Molecular Biology, vol. 1896,
https://doi.org/10.1007/978-1-4939-8931-7_12,

senescent cells in vitro and in vivo, with high specificity and sensitivity [8]. GL13 is a biotinylated Sudan Black-B (SBB) chemical analog (commercially available as SenTraGor™ by Arriani Pharmaceuticals Greece, Catalog number: AR8850040-AR8850080). GL13 interacts potently and specifically with lipofuscin and can be detected via an antibody-mediated chromogenic or fluorescent assay [8–11]. As a result, the application of GL13 outperforms most of the available and widely used senescent cell-staining methods with respect to their technical challenges, inherent limitations and systematic errors [8]. Interestingly, unprecedented quantification capacities also emerge, as shown herein. The currently described protocol represents an advancement rendering lipofuscin levels measurable in biological fluids. More specifically, we present a novel quantitative detection method of soluble or extracted lipofuscin levels in cell culture supernatants, body fluids and tissue homogenates that utilizes an antibody-mediated chemiluminescence assay.

Lipofuscin is a nondegradable substrate of metabolism that accumulates in cells due to impaired mitochondrial/lysosome (mitochondrial–lysosomal axis theory) and proteasome function, upon stress or cellular damage [12–20]. Stressed or damaged cells have ceased to proliferate and are therefore not able to degrade this substrate by cell division [17, 20]. The bulk mass of this heterogeneous material consists of oxidized proteins/lipoproteins, oxidized lipids and metals that become resistant to hydrolysis by lysosomal enzymes [17–19]. Lipofuscin is not inactive and harmless but harbors detrimental properties. Firstly, lipofuscin accumulation is known to reduce proteostasis and, particularly, the proteasomal activity, thus inhibiting the effective turnover of modified/oxidized proteins [17, 19, 21]. Secondly, it facilitates production of reactive oxygen species (ROS) via the Fenton reaction, mediated by its integrated redox-active metals [17, 19, 21]. Together, these lead to increased formation of oxidized intracellular molecules which, in turn, further promote lipofuscin aggregation in a positive feedback loop [17, 18, 21]. Based on the above, intracellular aggregation of lipofuscin signifies an impaired cellular status and deregulated homeostasis.

The quantification of lipofuscin is regarded as being of high importance for a wide range of life sciences and related disciplines. Lipofuscin levels seem to provide a lifetime history of cumulative exposure to metabolic stress and, thus, are directly related to the aging process and bear pathophysiological relevance [19, 21–23]. Increasing evidence supports a linear correlation of lipofuscin levels with age and age-related diseases [19, 21, 24]. This is rather well anticipated given that the number of senescent cells in tissues and organs increases with age as stress and damage accumulates [3–7, 20]. Interestingly, some age determination methods of organisms based on the quantification of lipofuscin have been described

[25–29], while a broad spectrum of age-related disorders, including Alzheimer's and Parkinson's disease, age-related macular degeneration, heart failure and others, have been associated with tissue and organ lipofuscin accumulation [19, 30–33]. Of note, early studies showed increased lipofuscin levels with age in peripheral human lymphocytes and plasma cells [34]. In addition, the presence of lipofuscin pigments was reported in erythrocyte membranes of Alzheimer's patients [35].

A number of studies provide indications that lipofuscin also exists in a soluble form in different body fluids. More specifically, Feng et al. claimed that lipofuscin concentrations detected in the plasma of human cases exhibited significantly higher levels than those observed in the saliva [36]. Similarly, detectable lipofuscin levels have also been reported in the plasma of mice [37]. Indirect evidence regarding the existence of lipofuscin in the plasma or blood serum based on its autofluorescence properties (soluble lipofuscin fluorophores) have also come in light [38–45]. Some of these reports focused on the putative correlation of lipofuscin levels in body fluids (mainly plasma) with age and different pathologies, in an attempt to establish a sensitive and reliable method for detecting and monitoring both aging and disease [38, 40, 42, 43, 46].

Yet a number of inherent difficulties are related with the measurement of lipofuscin to a good precision. Lipofuscin composition varies considerably between different tissues, organs, and species, thus leading to differences in distribution, staining, solubility, and enzymatic activity [47–49]. Additionally, this complicated mixture of oxidized macromolecules exhibits autofluorescent properties that possibly rely on Schiff bases formed by reactions between carbonyls and amino residues [18]. Broad deviations in excitation and emission (wavelengths ranging from 320 to 480 nm and from 460 to 630 nm, respectively) pose serious difficulties to methods based on direct spectroscopic characterization [14, 24, 50]. As a result, both the accuracy and the credibility of the available quantification methods to date, most of which rely mainly on lipofuscin autofluorescence, have received severe criticism.

Based on the excellent specificity of GL13 reagent, we describe a rapid, highly specific and precise protocol for detecting and measuring soluble lipofuscin levels in cell culture supernatants, body fluids as well as cell and tissue homogenates. In brief, lipofuscin is initially isolated from the studied biological samples according to the modified Folch extraction method [51], resuspended and treated with GL13 to saturation. Then, a primary anti-biotin antibody is applied and after incubation, a secondary antibody is used for detecting the lipofuscin–GL13 complex via a chemiluminescence reaction. Finally, lipofuscin levels are quantified on the basis of the resulting signal intensity (*see* Fig. 1). For determining the crude lipofuscin content of analyzed samples, luminescence is measured and signal intensity is matched with the

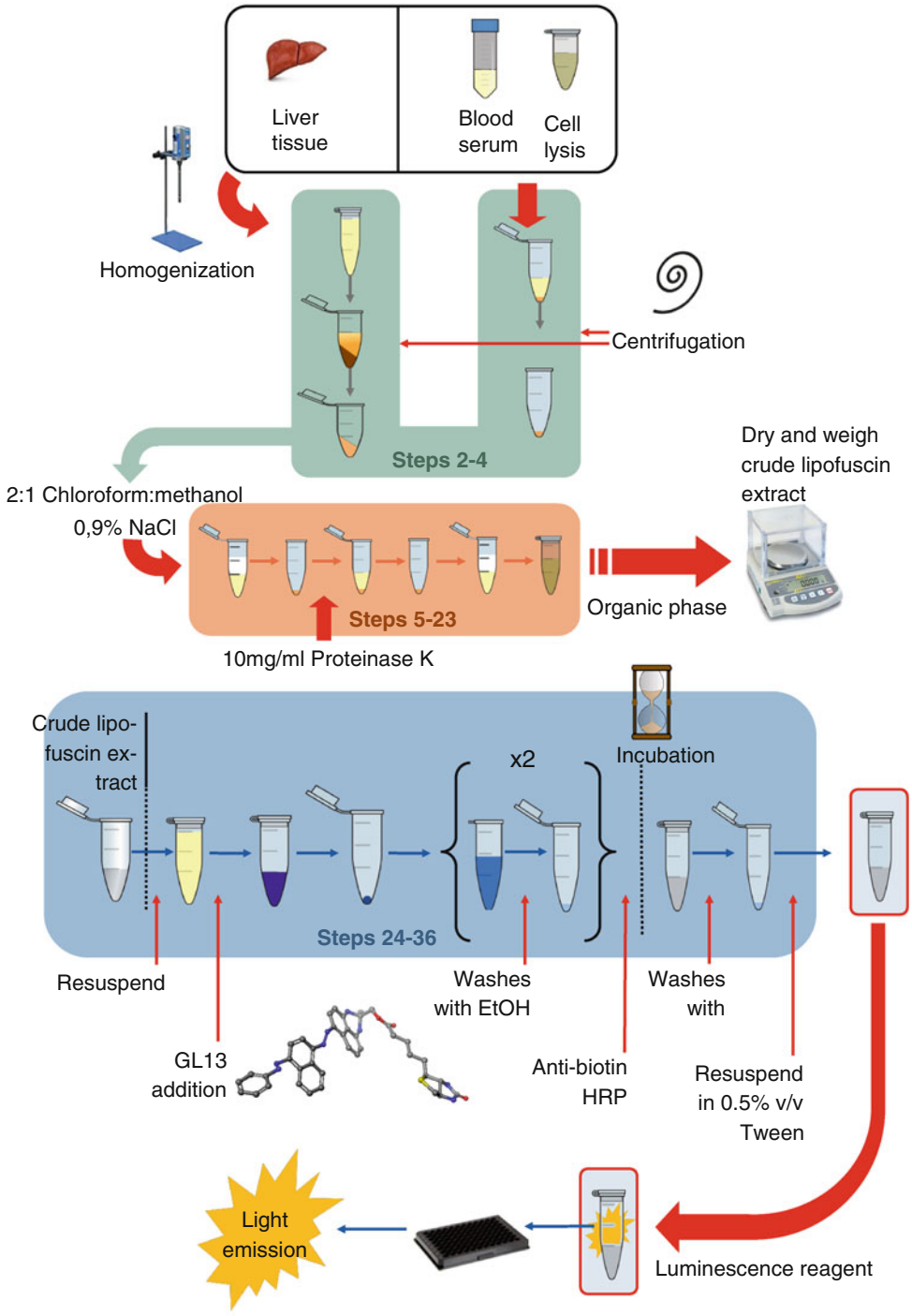

Fig. 1 Schematic workflow of lipofuscin isolation and detection procedures using different biological specimens. A diagram depicting key components of the protocol, as described in experimental procedure. Lipofuscin is isolated from homogenized human liver tissue, human blood serum, and cell lysates using chloroform–methanol and 10 mg/ml proteinase K incubation and centrifugation. Lipofuscin is dissolved in

corresponding values of a calibration curve created by following a similar protocol with the exception of lipofuscin being extracted from fresh aged human liver tissue. While in the young samples, lipofuscin levels were low [Relative Light Units (RLU): 10-471], in those obtained from aged individuals, we observed a 7.6-fold increase in measurement (RLU: 486-3.252). These findings not only provide an indication of the baseline levels of lipofuscin in humans (young cases) and of its distribution in elderly individuals, but also clearly confirm the linear correlation between lipofuscin and age, further denoting its putative role as a biomarker for monitoring the aging process (*see* Fig. 2). A stepwise scheme has been applied for validating the protocol (*see* Fig. 3). First, cell extracts from cellular models with established senescence and their corresponding, senescence-negative controls were analyzed and differences in lipofuscin levels were measured (*see* Fig. 3). Measurements showed a significant increase in soluble lipofuscin levels in the samples obtained from senescent cells in comparison to those from untreated cells [HBEC-CDC6 Tet-Off vs HBEC-CDC6 Tet-On (6 days on induction), Saos-2 $p21^{WAF1/Cip1}$ Tet-Off vs Saos-2 $p21^{WAF1/Cip1}$ Tet-On (10 days induction)] (*see* Figs. 1 and 3). Subsequently, we extracted intracellular lipofuscin from the same cellular models and repeated the quantification assay (*see* Fig. 1). The protocol was then implemented for determining lipofuscin in blood sera from young (controls) and aged but "healthy" individuals as well as patients suffering from different kinds of pathologies. These included heart failure, neurodegenerative disorders (dementia), rheumatoid arthritis and cancer (*see* Table 1, Fig. 4a, b). Clinical sample collection and their experimental use were approved by the Bio-Ethics Committee of Medical School of Athens, in accordance with the Declaration of Helsinki and local laws and regulations. Written consent was also obtained from the patients. As an additional level of validation, lipofuscin levels measured in human tissues by the herein presented GL13-based chemiluminescence assay were correlated with lipofuscin concentration in the same tissues as assessed by the hybrid histochemistry–immunohistochemistry method [8] (*see* Fig. 5). Further control experiments included electron microscopy in order to verify that the extracted material exhibits morphological features similar to those described for isolated lipofuscin [54] (*see* Fig. 6).

The current method allows for an accurate estimation of soluble lipofuscin levels practically in any biological material. Given that

Fig. 1 (continued) organic phase, which is evaporated and weighed. Crude lipofuscin extract is resuspended in 1% v/v Tween 20/TBS. After centrifugation, the pellet is resuspended in EtOH 50% and the biotin-conjugated SBB analog (GL13) is added. GL13 binds to lipofuscin and the anti-biotin HRP antibody binds to the biotin moiety of GL13. HRP will react upon addition of luminescent substrate (luminol and H_2O_2) and light will be emitted. Concentration of lipofuscin in each sample is linearly proportional to light intensity

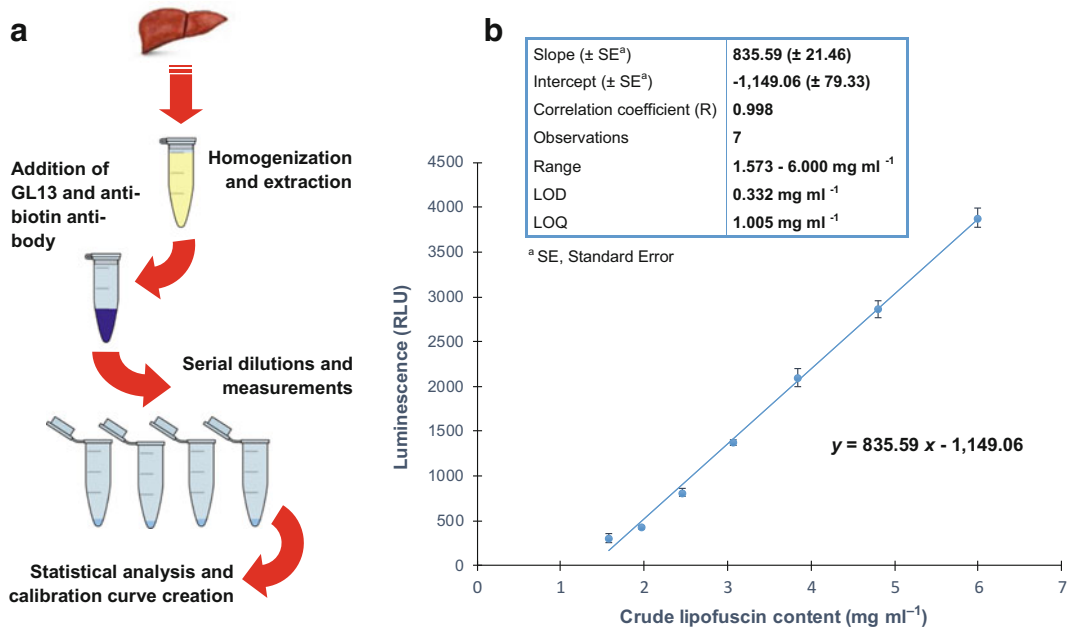

Fig. 2 (**a**) Schematic summary of the procedure implemented to create a calibration curve. The calibration curve is constructed by following **steps 1-III** to **34** as described in experimental procedure, with the exception of preparing 5–7 serial dilutions of the sample obtained after **step 31** (dilution of each sample by 20% using 0.5% v/v Tween 20/TBS buffer). Measurements are recorded on an Excel spreadsheet and linear regression analysis is performed. Determination of back calculated values may be assisted by using the Data analysis add-in of Microsoft Excel and implementing manual functions. (**b**) The calibration curve for the determination of crude lipofuscin content in liver tissue samples along with related parameters and metrics. Linear regression analysis has been performed with no weighting factors, while the 0.0 point was neither included nor the curve forced through it upon fitting (Error bars, 95% confidence intervals; $n = 3$). The LOD and LOQ values are determined as $3.3 \times S_Y$/slope and $10 \cdot S_Y$/slope, respectively, where S_Y is the standard error of the response at low concentration. Back calculated values exhibited error values lower than 10.6%, demonstrating the validity of the calibration curve

lipofuscin concentration has often been associated to age and various age-related diseases [19, 25–33], the applicability domain of the protocol presented herein is particularly broad. The determination of lipofuscin distribution in human body fluids according to age, gender or any other epidemiological characteristic is now feasible in the general population. To our knowledge, this issue has not been sufficiently addressed in the past. Furthermore, the method itself may well promote biomedical and clinical investigations on whether soluble lipofuscin levels could serve as a putative biomarker of aging and/or disease. In this context, wide-scale screening of populations, as well as groups of differences in age and disease, is likely to assist in determining cases that are at "risk," despite a "young" and/or "healthy" phenotype, hence providing a new tool for early detection. Additionally, monitoring lipofuscin in the blood serum could provide valuable information on patient

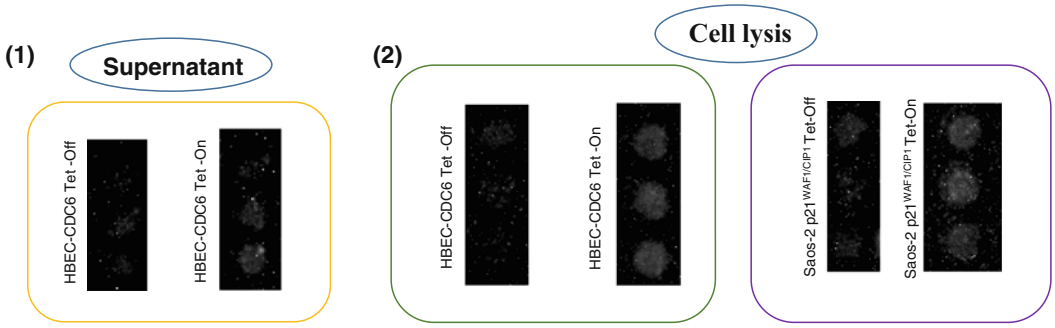

(3)

	Supernatant		Cell extract			
	HBEC-CDC6 Tet-Off	HBEC-CDC6 Tet-On	HBEC-CDC6 Tet-Off	HBEC-CDC6 Tet-On	Saos-2 p21$^{WAF1/CIP1}$ Tet-Off	Saos-2 p21$^{WAF1/CIP1}$ Tet-On
Measurement 1	68	279	171	1005	212	1466
Measurement 2	89	317	153	1068	143	1789
Measurement 3	97	364	146	1221	167	1235
Average	84.66666667	320	156.6666667	1098	174	1496.666667
Number of cases	3	3	3	3	3	3
StDev	14.97776129	42.57933771	12.89702808	111.0810515	35.02855978	278.2702523
StErr	8.469556233	27.98681809	6.99825567	76.42484443	22.64761181	194.6454621

Fig. 3 Lipofuscin detection with GL13 and chemiluminescence after isolation from cell culture supernatant and cell lysis. (1) Images showing chemiluminescence intensity from supernatant of HBEC-CDC6 Tet-Off and Tet-On cell lines. (2) Images showing chemiluminescence intensity of cell extracts derived from cellular models with established senescence (HBEC-CDC6 Tet-On and Saos-2 p21^{WAF-1} Tet-On) in comparison with their corresponding, senescence-negative controls (HBEC-CDC6 Tet-Off and Saos-2 p21^{WAF-1} Tet-Off). (3) Table showing the values and the statistical data of chemiluminescence intensity measurements in each group and sample

Table 1
Groups of human specimens used for measuring soluble lipofuscin levels along with their health condition and number of individual samples

Biological specimen	Condition/disease (age, in years)	Number of samples
Blood serum	Young healthy (21–25)	10
Blood serum	Aged healthy-MRMF[a] (65–94)	10
Blood serum	Heart failure (62–85)	10
Blood serum	Neurodegenerative diseases/dementia (49–94)	10
Blood serum	Rheumatoid arthritis (27–67)	10
Blood serum	Cancer (55–83)	10
Follicular fluid	Infertile women (33–46)	5
Follicular fluid	Oocyte donors (normal) (23–27)	5

[a]Medical record plus medications-free

outcome, recurrence of disease and response to therapeutic interventions toward a personalized medicine strategy. Moreover, new drug leads could be screened in a high-throughput manner for their effect on cellular senescence, thus facilitating discovery of senolytics, an emerging and highly promising class of bioactive compounds [55]. Other potential applications might involve the food industry, where monitoring superior quality properties such as

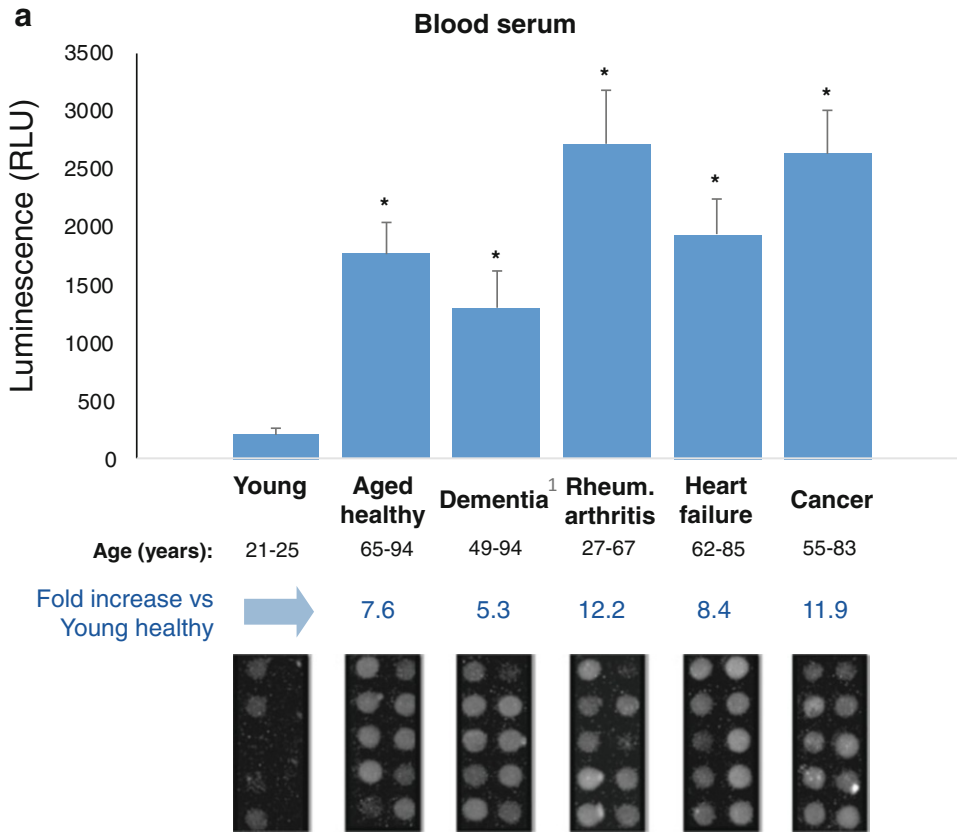

Fig. 4 (**a**) Graph showing luminescence intensity of serum samples derived from different groups of individuals ($n = 10$ in each group) after treatment with GL13. Clear differences in lipofuscin levels are evident between samples from young and aged "MRMF" individuals but also between young healthy individuals and others falling under various pathological entities. The measurements in aged and pathological samples correspond to increase of lipofuscin levels ranging between 5.3-fold and 12.2-fold in comparison to young healthy samples (Error bars, Standard Error; *, $P < 0.05$). (**b**) Graph showing chemiluminescence intensity of follicular fluid samples derived from different groups of individuals ($n = 5$ in each group) after treatment with GL13. It has been previously shown that an altered redox state of follicular fluid albumin influences the viability of aspirated human oocytes [52]. Lipofuscin accumulation in the form of inclusions within oocytes is associated with a significantly reduced fertilization rate and unfavorable blastocyst development [53]. Clear differences in lipofuscin levels are evident between samples from normal oocyte donors and infertile women. Our results confirmed this notion in follicular fluid, showing an eightfold increase in lipofuscin among infertile women compared to normal donors. The measurements obtained from these samples correspond to a 7.5-fold increase of lipofuscin levels in comparison to normal donor samples (Error bars, Standard Error; *, $P < 0.05$)

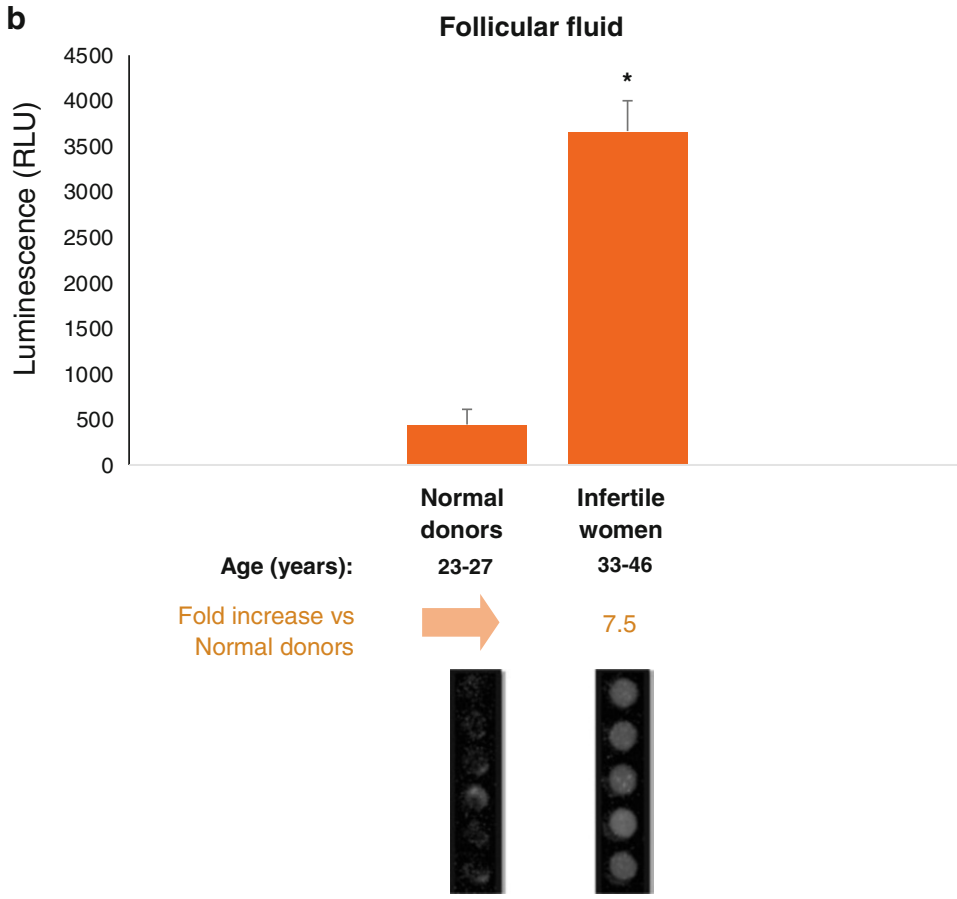

Fig. 4 (continued)

age, freshness and health of consumable organisms are of great commercial importance. A similar approach has been followed in demographic analyses of economically important species (e.g., the blue crab *Callinectes sapidus*) by measuring extracted fluorescence [29], yet with the drawbacks of conventional methodologies [28, 56, 57]. Finally, the method could be exploited by the cosmetics industry in order to monitor the efficiency and response to rejuvenation-treatments and antiaging products.

In only a limited number of available reports, soluble lipofuscin levels were measured using a spectrophotometer according to the Tsuchida method that is based on lipofuscin autofluorescence in the blood serum. The concentration of fluorophores is expressed in arbitrary units in comparison to the fluorescence of a quinine sulphate reference [29, 40, 57]. The major disadvantage of this approach is that, apart from lipofuscin, several other fluorophores exist in the blood and its derivatives, as is the case with other tissues. These fluorophores include a wide spectrum of molecules such as amino acids (tryptophan) and proteins (albumin, enzymes and

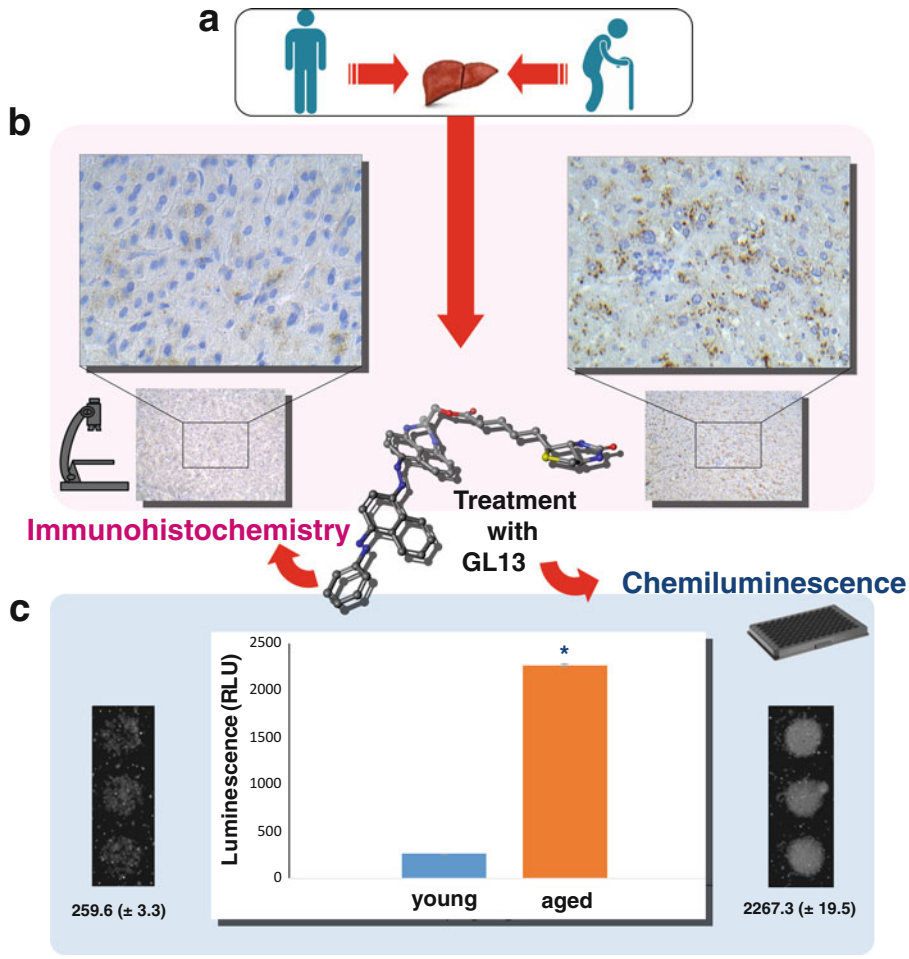

Fig. 5 Schematic illustration summarizing two alternative procedures that can depict lipofuscin accumulation in human liver tissue with the use of the biotinylated SBB analog GL13. (**a**) Human liver tissue samples were isolated from young (left) and aged (right) individuals. (**b**) Part of the tissue was formalin fixed, paraffin embedded (FFPE) and used for light microscopy. The histochemical–immunohistochemical assay was performed in FFPE tissues using GL13, showing evident differences in lipofuscin levels between young and aged samples at the 100× and 400× magnifications. (**c**) Another part of each human liver tissue sample was homogenized, and lipofuscin was isolated and treated with GL13. The resulting luminescence was measured as described in experimental procedure. The analysis shows an eightfold increase of lipofuscin levels in young compared to aged liver tissue samples, in agreement with the microscopic observations (measurements in Relative Light Units ± Standard Error, $n = 3$; *, $P < 0.05$)

others), porphyrins, carotenoids, vitamins (vitamin A, riboflavin, thiamine), pyridine nucleotides (NADH/NAD^+, NADPH/$NADP^+$), pyridoxic acid lactone, pyridoxal phosphate Schiff bases, and protein-bound bilirubin [23, 57–59]. Given that their fluorescence spectra are highly similar to those of lipofuscin, they may well interfere with measurements, thus producing serious analytical errors. Therefore, the specificity of the aforementioned method in

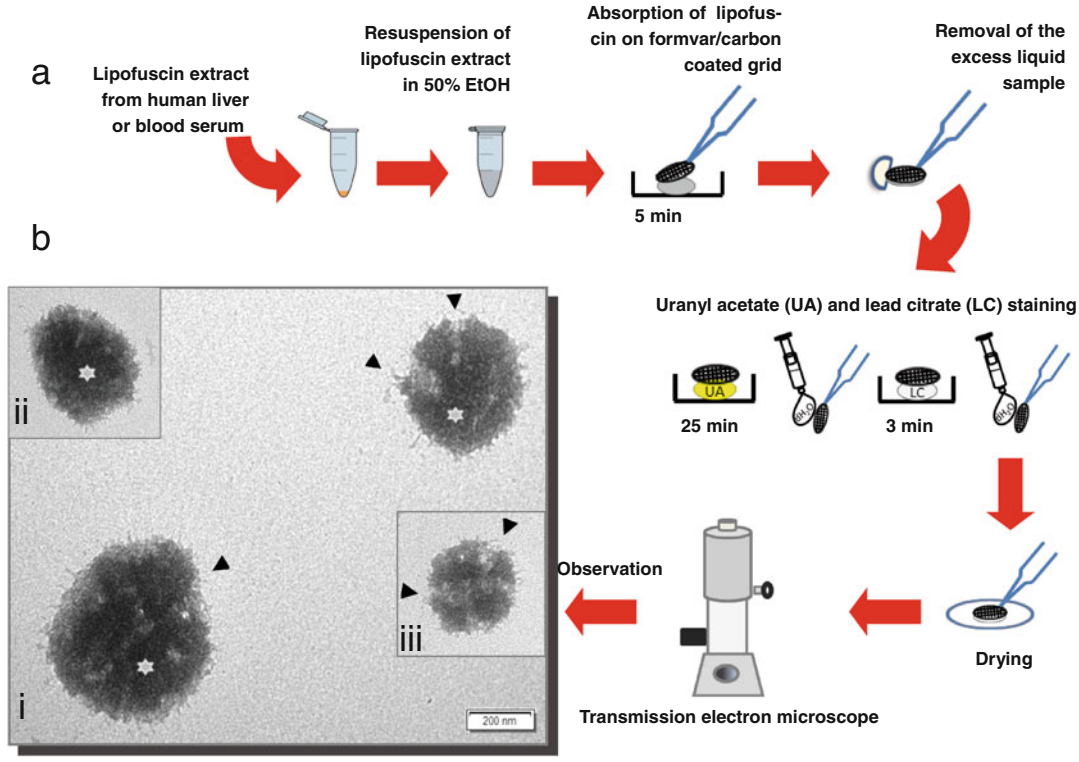

Fig. 6 Lipofuscin extract observation under a transmission electron microscope (TEM). (**a**) Diagrammatic representation of the procedure followed for the preparation and positive staining of the lipofuscin sample on a formvar/carbon coated grid. The grid with the absorbed/stained lipofuscin sample was observed under a TEM operating at 80 KV and equipped with a digital camera. (**b**) Transmission electron micrographs of lipofuscin formations exhibiting the same morphology whether extracted from human liver tissue (**i**) or from blood serum (**ii**, **iii**). Lipofuscin formations were characterized by small electron-lucent areas (arrowheads) indicating the localization of lipid components, and wide electron-dense areas exhibiting very fine vacuolization (asterisks). Scale bar: 200 nm

determining lipofuscin levels has been strongly questioned. In addition, the estimation of lipofuscin levels is rather relative and lacks accuracy when using a standard curve based on a quinine sulphate reference [29, 40, 57]. In line with the above, fluorimetry has been extensively criticized when exploited in marine biology for determining the age of aquatic organisms. The main concerns raised were the absence of specificity which is not counterbalanced by high-throughput assays, the poor correlation between extracted fluorescence and in situ lipofuscin levels, and the lack of evidence that normalization to cellular protein content actually leads to a reliable lipofuscin assay [56]. A flow-cytometric (FACS) approach for the quantification of extractable neurolipofuscin again exhibited fundamental precision pitfalls [22]. Our proposed method specifically detects lipofuscin by exploiting the unique features of GL13 in a rapid, simple and straightforward manner. Electron microscopy

analysis confirmed the morphological characteristics of lipofuscin in the extracted material [54] (*see* Fig. 6). Moreover, the calibration curve presented herein is designed to directly correlate crude lipofuscin concentration with its corresponding chemiluminescence signal, thus enabling self-consistent, precise and convenient measurements in a range of different samples (*see* Fig. 2). Lastly, a strong correlation between chemiluminescence measurements (amount of crude lipofuscin) and in situ lipofuscin concentration was observed in control experiments (*see* Fig. 5).

Another approach described by Feng et al. used an enzyme-linked immunosorbent assay (ELISA) kit provided by the Shanghai Huyu Biological Technology Co. Ltd. to estimate lipofuscin levels in human saliva and plasma [36]. A comparison with our method is not feasible since no details regarding the kit or its composition (particularly which component of lipofuscin the applied primary antibody reacts against) are available in the literature. Since its publication in 2015, and to the best of our knowledge, the above method and its accompanying kit have never been used elsewhere by the same or other researchers. Similar issues exist with the Human Quantitative Competitive ELISA Lipofuscin (LPF) kit distributed by MyBioSource (catalog # MBS7230952). Since the composition of lipofuscin varies considerably among different tissues and species [47–49], particularly with respect to the protein fraction, the ELISA assay raises serious concerns about the lipofuscin module targeted by the primary antibody and, to an extent, about the specificity, sensitivity, accuracy and suitability of the overall method. No information on this matter exists in the literature.

2 Materials

2.1 Lipofuscin Isolation

1. Chloroform.
2. Methanol.
3. 0.9% sodium chloride in dH_2O.
4. 10 mg/ml proteinase K.
5. 20× TBS. Dissolve 121 g of Tris ultrapure in 800 ml of dH_2O. Adjust the pH to 7.4 with concentrated HCl.
6. 1× TBS in dH_2O.
7. 50% (vol/vol) ethanol absolute in 1× TBS.
8. Greiner Microlon Black 96-well plate.
9. Centrifuge.
10. Homogenizer.
11. Rotary evaporator with vacuum controller and vacuum pump.

12. High vacuum pump.
13. Ultrasonic bath.
14. Analytical balance.
15. 50 ml round bottom flask.

2.2 Lipofuscin Detection Using GL13 and Chemiluminescence

1. 80 mg SenTraGor. Dissolve 80 mg of SenTraGor in 14.5 ml 100% ethanol and incubate for 120 min in water bath at 37 °C.
2. Chemiluminescence Reagent. Add equal volumes of Lumi-GLO Reagent A and Reagent B.
3. Anti-biotin HRP-linked antibody diluted 1:1000 in 0.1% v/v Tween 20/TBS.
4. Tween 20.
5. Fluorchem HD2 system equipped with a CCD camera.

2.3 Positive Staining of Lipofuscin for Electron Microscopy

1. Uranyl acetate.
2. Lead citrate.
3. Formvar/carbon-coated copper grids, 200 mesh.
4. Tweezers, antimagnetic stainless steel, style #5.
5. Grid-box for storage of grids.
6. Electron microscope.

3 Experimental Procedure

3.1 Lipofuscin Isolation (Timing: 4–5 h)

1. *I. Human blood serum*: Transfer 500 μl of serum in 1.5 ml Eppendorf (*see* **Notes 1** and **2**, Table 2).
   II. Cell lysis: Incubate cell pellet with Co-IP lysis buffer for 60 min at 4 °C.
   III. Liver tissue: Homogenize tissue using PBS 1× 2–3 times for 20–30 s each, pausing for 10–15 s between each homogenization and placing samples on ice.
2. Centrifuge at 6–8 °C for 10 min at 232 × *g*.
3. Transfer supernatant in 1.5 ml eppendorf.
4. Centrifuge at 6–8 °C for 10 min at 7400 × *g* to sediment lipofuscin (*see* **Note 3**).
5. Resuspend the pellet in a mixture 2:1 chloroform and methanol (*see* **Notes 4** and **5**).
6. Dilute sample by 20% using a solution of 0.9% NaCl in distilled water and vortex.
7. Use ultrasonication for 1 min to enhance resuspension and transfer lipofuscin to organic phase (*see* **Notes 6** and **7**, Table 2).

Table 2
Troubleshooting

Step	Problem	Possible reason	Solution
1 I	Low amount of pellet	Low lipofuscin content in blood serum	Increase volume of blood serum sample
7	Large amounts of lipofuscin trapped in intermediate phase	Sonication conditions not optimal	Increase sonication time. This step is crucial to transfer chloroform-insoluble lipofuscin components in organic phase
23	Solvent is not completely evaporated under a 474 mbar vacuum	Traces of the aqueous phase have been isolated along with the organic phase	Gradually increase vacuum in rotary evaporator down to 72 mbar and extend evaporation time
24	Incomplete precipitation of lipofuscin	Speed of centrifugation	Increase centrifuge acceleration up to 7400 × *g*
25	Amount of GL13 not sufficient to saturate lipofuscin content of sample	High levels of lipofuscin in analyzed sample	Increase volumes of GL13 stock solution and EtOH 50% resuspension solution in same proportions
32	Poor resuspension of crude lipofuscin extract in 0.5% v/v Tween 20/TBS buffer	Excess amount of lipofuscin	Incubate for 5–10 min in water bath at 37 °C

8. Incubate the samples for 15 min at room temperature with gentle shaking.
9. Centrifuge at 3700 × *g* for 10 min at 6–8 °C.
10. Remove the aqueous (upper) phase using a pipette.
11. Transfer and keep organic phase in 1.5 ml eppendorf.
12. Incubate intermediate phase with 10 mg/ml Proteinase K for 30 min at 37 °C with gentle shaking (*see* **Note 8**).
13. Centrifuge at 3700 × *g* for 10 min at 6–8 °C.
14. Discard supernatant and resuspend pellet in a mixture 2:1 chloroform: methanol (*see* **Note 4**).
15. Dilute by 20% using 0.9% NaCl in distilled water and vortex.
16. Incubate the mixtures for 15 min at room temperature with gentle shaking.
17. Centrifuge at 3700 × *g* for 10 min at 6–8 °C.
18. Using a pipette, remove (upper) aqueous phase (*see* **Note 9**).
19. Transfer and keep organic phase in 1.5 ml eppendorf.
20. Merge organic phase samples from **steps 11** and **19**, transfer into a preweighed 50 ml round bottom flask and evaporate solvent using a rotary evaporator apparatus and a heating bath at 37 °C (*see* **Notes 10** and **11**).

21. Connect the round bottom flask to a high vacuum pump for 10 min.
22. Use an analytical balance to weigh the spherical flask and determine the weight of the dried crude lipofuscin content.
23. Resuspend crude lipofuscin extract in 1% v/v Tween/TBS using ultrasonication for 5–10 min at 37 °C (*see* **Notes 12** and **13**, Table 2).

3.2 Lipofuscin Detection Using GL13 and Chemiluminescence (Timing: 4–5 h)

24. Centrifuge at 7400 × *g* for 10 min at 6–8 °C (*see* **Note 14**, Table 2).
25. Resuspend pellet in 200 µl EtOH 50% and add 7.5 µl of the GL13 stock solution. Incubate for 8 min at room temperature with gentle shaking (*see* **Notes 15** and **16**, Table 2).
26. Centrifuge at 7400 × *g* for 10 min at 6–8 °C.
27. Wash with 500 µl of EtOH 50% and centrifuge at 6–8 °C for 10 min at 7400 × *g* (*see* **Note 17**).
28. Resuspend pellet in 100 µl of TBS 1×.
29. Add the anti-biotin HRP-linked antibody diluted 1:1000 in 0.1% v/v Tween 20/TBS to each sample. Incubate for 120 min at room temperature with gentle shaking (*see* **Note 18**).
30. Centrifuge at 7400 × *g* for 10 min at 6–8 °C.
31. Wash with 200 µl TBS 1× and centrifuge at 7400 × *g* for 10 min at 6–8 °C. Repeat this step twice.
32. Resuspend the lipofuscin pellet in 90 µl 0.5% v/v Tween 20/TBS and transfer the solution in a 96-well plate (*see* **Note 19**, Table 2).
33. Mix equal volumes of chemiluminescence substrate Lumiglo® Reagent A and B in a plastic tube protected from light (*see* **Note 20**).
34. Add 10 µl (dilution factor: 1/10) of chemiluminescence solution in every sample-containing well.
35. After 1 min approximately, measure emitted light using a multiplex chemiluminescence imaging system.
36. Quantify luminescence intensity with AlphaView software v1.3.0.7.

3.3 Positive Staining of Lipofuscin for Electron Microscopy (Timing: 1 h)

1. In samples derived from **step 19** of the experimental procedure, add 20 µl EtOH 50% and resuspend.
2. Place drops of 5–10 µl of liquid sample onto a sheet of Parafilm in a petri dish.
3. Place formvar/carbon-coated 200 mesh copper grids on drops of liquid sample and allow to absorb for 5 min at RT.

4. Wick away excess liquid sample from each grid applying carefully the torn edge of Whatman filter paper at the edge of the grid.
5. Immediately float the grids on filtered drops (20–30 μl) of 7% uranyl acetate (aqueous solution) onto a sheet of Parafilm in a petri dish. Stain for 25 min at room temperature in the dark.
6. Wash grids under a stream of distilled water.
7. Drain the grids.
8. Float the grids on filtered drops (20–30 μl) of 0.4% lead citrate (aqueous solution) onto a sheet of Parafilm in a petri dish. Place NaOH tablets or 10 N NaOH solution droplets around the Parafilm sheet in the petri dish to create a dry alkaline atmosphere, lacking CO_2. Stain each grid for 3 min at room temperature (*see* **Note 21**).
9. Immediately apply very short (~2 s) washes of the grids with 0.02 N NaOH solution and then wash thoroughly under a stream of distilled water.
10. Dry the grids and store them in a grid box.
11. Observe the grids under a transmission electron microscope.

4 Notes

General: Precise and careful handlings during various steps of the protocol are required.

1. Fresh—or stored for a short period of time—biological material is preferred. It has been shown that during long term storage, blood derivatives may lose their osmotic, hemostatic, immunologic and other physiological properties, as more proteins included in the samples tend to transform into lipofuscin with time [60].
2. Low amount of pellet indicates low lipofuscin content in the sample. To overcome this, increased sample volume should be analyzed.
3. The molecular weight of lipofuscin is similar to that of mitochondria.
4. Chloroform and methanol are hazardous chemicals. Avoid contact with skin, eyes and airways.
5. The usage of chloroform when extracting lipofuscin is associated with a variety of health, security, and regulatory issues. Dichloromethane/methanol could replace the employed chloroform/methanol steps in order to bypass these issues [61].
6. Ultrasonication contributes in dissolving chloroform-insoluble lipofuscin components.

7. If large amounts of lipofuscin are trapped in intermediate phase increase the duration of sonication. This step is crucial to transfer chloroform-insoluble lipofuscin components into the organic phase.
8. Proteinase K will release lipids from lipoprotein structures in order to enable quantification of chloroform-insoluble lipofuscin.
9. It is important to remove the aqueous phase without entering the organic phase to avoid decrease in lipofuscin levels.
10. Chloroform should be totally evaporated. If possible, use a rotary evaporator connected to a vacuum controller and set the cut-off value at 474 mbar. Evaporation time depends on total solvent volume.
11. If the solvent is not completely evaporated under 474 mbar vacuum, probably due to traces of the aqueous phase that have been isolated along with the organic phase, gradually decrease vacuum in rotary evaporator down to 72 mbar and extend evaporation time.
12. It is important to ensure that lipofuscin is entirely resuspended.
13. Samples can be stored for 12 h at 4 °C.
14. Upon incomplete lipofuscin precipitation increase centrifuge acceleration up to 7400 × *g*.
15. The GL13 stock solution should be passed through a 0.22-μm filter before use. For further details, see Evangelou et al. [8].
16. GL13 amounts should always be adjusted in a manner that ensures sufficient saturation of sample lipofuscin content.
17. Repeat this step several times (2–3 minimum). Observe color of supernatant. Washing has been sufficiently performed when supernatant is clear and transparent, without any blue haze or floating particles of SBB analog.
18. Avoid repeated freeze–thaw cycles of the anti-biotin HRP conjugate antibody which may result in reduced activation of the HRP enzyme.
19. Poor resuspension of crude lipofuscin extract in 0.5%v/v Tween 20/TBS buffer indicates excess in lipofuscin amounts. To address this issue incubate for 5–10 min in water bath at 37 °C.
20. The volume of chemiluminescence substrate depends on the number of samples.
21. Avoid breathing over the grids in order to prevent the formation of lead precipitates due to the addition of CO_2 in the atmosphere.

Acknowledgments

We would like to thank Dr. Alexandros Papalampros and Dr. Dimitrios Papadopoulos for providing material for this investigation. This work was financially supported by the "SYNTRAIN" ITN Horizon 2020 Grant No 722729, the NKUA SARG grants 70/3/12128, 70/3/8916, 70/3/1135 and the Welfare Foundation for Social & Cultural Sciences (KIKPE) Greece.

Conflict of interest:
The authors wish to declare no conflict of interest.
Patent pending: UK Patent Application No GB1803531.1.

References

1. Georgakopoulou EA, Tsimaratou K, Evangelou K et al (2013) Specific lipofuscin staining as a novel biomarker to detect replicative and stress-induced senescence. A method applicable in cryo-preserved and archival tissues. Aging (Albany NY) 5:37–50
2. Evangelou K, Gorgoulis VG (2017) Sudan Black B, The specific histochemical stain for lipofuscin: a novel method to detect senescent cells. Methods Mol Biol 1534:111–119
3. Bartkova J, Rezaei N, Liontos M et al (2006) Oncogene-induced senescence is part of the tumorigenesis barrier imposed by DNA damage checkpoints. Nature 444:633–637
4. Gorgoulis VG, Halazonetis TD (2010) Oncogene-induced senescence: the bright and dark side of the response. Curr Opin Cell Biol 22:816–827
5. Halazonetis TD, Gorgoulis VG, Bartek J (2008) An oncogene-induced DNA damage model for cancer development. Science 319:1352–1355
6. Herbig U, Ferreira M, Condel L et al (2006) Cellular senescence in aging primates. Science 311:1257
7. Lopez-Otin C, Blasco MA, Partridge L et al (2013) The hallmarks of aging. Cell 153:1194–1217
8. Evangelou K, Lougiakis N, Rizou SV et al (2017) Robust, universal biomarker assay to detect senescent cells in biological specimens. Aging Cell 16:192–197
9. Galanos P, Vougas K, Walter D et al (2016) Chronic p53-independent p21 expression causes genomic instability by deregulating replication licensing. Nat Cell Biol 18:777–789
10. Komseli ES, Pateras IS, Krejsgaard T et al (2018) A prototypical non-malignant epithelial model to study genome dynamics and concurrently monitor micro-RNAs and proteins in situ during oncogene-induced senescence. BMC Genomics 19:37
11. Barbouti A, Evangelou K, Pateras IS et al (2018) In situ evidence of cellular senescence in Thymic Epithelial Cells (TECs) during human thymic involution. Mech Ageing Dev. pii:S0047-6374(17)30300-7
12. Ivy G, Kanai S, Ohta M et al (1988) Lipofuscin-like substances accumulate rapidly in brain, retina and internal organs with cysteine protease inhibition. Adv Exp Med Biol 266:31–45
13. Ivy G, Roopsingh R, Kanai S et al (1996) Leupeptin causes an accumulation of lipofuscin-like substances and other signs of aging in kidneys of young rats: further evidence for the protease inhibitor model of aging. Ann N Y Acad Sci 786:12–23
14. Brunk UT, Terman A (2002) Lipofuscin: mechanisms of age-related accumulation and influence on cell function. Free Radic Biol Med 33:611–619
15. Terman A, Gustafsson B, Brunk UT (2006) The lysosomal-mitochondrial axis theory of postmitotic aging and cell death. Chem Biol Interact 163:29–37
16. Terman A, Kurz T, Navratil M et al (2010) Mitochondrial turnover and aging of long-lived postmitotic cells: the mitochondrial-lysosomal axis theory of aging. Antioxid Redox Signal 12(4):503–535
17. Höhn A, Grune T (2013) Lipofuscin: formation, effects and role of macroautophagy. Redox Biol 19(1):140–144

18. Jung T, Höhn A, Grune T (2014) The proteasome and the degradation of oxidized proteins: partII protein oxidation and proteasomal degradation. Redox Biol 2:99–104
19. König J, Ott C, Hugo M et al (2017) Mitochondrial contribution to lipofuscin formation. Redox Biol 11:673–681
20. Korolchuk VI, Miwa S, Carroll B et al (2017) Mitochondria in cell senescence: is mitophagy the weakest link? EBioMedicine 21:7–13
21. Gaspar J, Mathieu J, Alvarez PJJ (2016) A rapid platform to generate lipofuscin and screen therapeutic drugs for efficacy in lipofuscin removal. Mater Meth Technol 10:1–9 ISSN 1314-7269
22. Sheehy MR (2002) A flow-cytometric method for quantification of neurolipofuscin and comparison with existing histological and biochemical approaches. Arch Gerontol Geriatr 34:233–248
23. Di Guardo G (2015) Lipofuscin, lipofuscin-like pigments and autofluorescence. Eur J Histochem 59:2485
24. Seehafer SS, Pearce DA (2006) You say lipofuscin, we say ceroid: defining autofluorescent storage material. Neurobiol Aging 27:576–588
25. Bluhm BA, Brey T (2001) Age determination in the Antarctic shrimp Notocrangon antarcticus (Crustacea: Decapoda), using the autofluorescent pigment lipofuscin. Mar Biol 138:247–257
26. Bluhm BA, Brey T, Klages M (2001) The autofluorescent age pigment lipofuscin: key to age, growth and productivity of the Antarctic amphipod *Waldeckia obesa* (Chevreux, 1905). J Exp Mar Bio Ecol 258:215–235
27. Cassidy KM (2008) Use of extractable lipofuscin as an age biomarker to determine age structure of ghost shrimp (*Neotrypaea californiensis*) populations in west coast estuaries. Dissertation. Oregon State University
28. Harvey HR, Secor DH, Ju SJ (2008) The use of extractable lipofuscin for age determination of crustaceans: reply to Sheehy. Mar Ecol Prog Ser 353:307–311
29. Puckett JB, Secor DH, Ju SJ (2008) Validation and application of lipofuscin-based age determination for Chesapeake Bay Blue Crabs *Callinectes sapidus*. Trans Am Fish Soc 137:1637–1649
30. Sparrow JR, Nakanishi K, Parish CA (2000) The lipofuscin fluorophore A2E mediates blue light induced damage to retinal pigmented epithelial cells. Invest Ophthalmol Vis Sci 41:1981–1989
31. Meredith GE, Totterdell S, Petroske E et al (2002) Lysosomal malfunction accompanies alpha-synuclein aggregation in a progressive mouse model of Parkinson's disease. Brain Res 956:156–165
32. Moreira PI, Siedlak SL, Wang X et al (2007) Increased autophagic degradation of mitochondria in Alzheimer disease. Autophagy 3:614–615
33. Nozynski J, Zakliczynski M, Konecka-Mrowka D et al (2013) Advanced glycation end products and lipofuscin deposits share the same location in cardiocytes of the failing heart. Exp Gerontol 48:223–228
34. Beregi E, Regius O (1983) Lipofuscin in lymphocytes and plasma cells in aging. Arch Gerontol Geriatr 2:229–235
35. Skoumalová A, Mádlová P, Topinková E (2012) End products of lipid peroxidation in erythrocyte membranes in Alzheimer's disease. Cell Biochem Funct 30:205–210
36. Feng FK, E LL, Kong XP et al (2015) Lipofuscin in saliva and plasma and its association with age in healthy adults. Aging Clin Exp Res 27:573–580
37. Wu CX, Wei XB (2006) Influence of effective parts of Zingiber officinale on senium of rats resulting from high fat die. J Shandong Med Coll 3:010
38. Hegedus ZL, Frank HA, Steinman TI et al (1988) Elevated levels of plasma lipofuscins in patients with chronic renal failure. Arch Int Physiol Biochim 96:211–221
39. Tsuchida M, Miura T, Mizutani K et al (1985) Fluorescent substances in mouse and human sera as a parameter of in vivo lipid peroxidation. Biochim Biophys Acta 834:196–204
40. Roumen RM, Hendriks T, de Man BM et al (1994) Serum lipofuscin as a prognostic indicator of adult respiratory distress syndrome and multiple organ failure. Br J Surg 81:1300–1305
41. Sutherland WH, Williams MJ, de Jong SA (2007) Plasma protein lipofuscin-like fluorophores in men with coronary artery disease treated with statins. Arch Med Res 38:757–763
42. Skoumalová A, Ivica J, Šantorová P et al (2011) The lipid peroxidation products as possible markers of Alzheimer's disease in blood. Exp Gerontol 46:38–42
43. Kuznetsov A, Frorip A, Maiste A et al (2015) Visible auto-fluorescence in biological fluids as biomarker of pathological processes and new monitoring tool. J Innov Opt Health Sci 8 (3):1541003–1541009

44. Tomečková V (2016) Monitoring of heart ischemia in blood serum. Spectral Anal Rev 4:11–22
45. Chmátalová Z, Vyhnálek M, Laczó J et al (2016) Analysis of lipophilic fluorescent products in blood of Alzheimer's disease patients. J Cell Mol Med 20:1367–1372
46. Madhuri S, Vengadesan N, Aruna P et al (2003) Native fluorescence spectroscopy of blood plasma in the characterization of oral malignance. Photochem Photobiol 78:197–204
47. Sheehy MR, Roberts BE (1991) An alternative explanation for anomalies in "soluble lipofuscin" fluorescence data from insects, crustaceans, and other aquatic species. Exp Gerontol 26:495–509
48. Yin D (1996) Biochemical basis of lipofuscin, ceroid, and age pigment-like fluorophores. Free Radic Biol Med 21:871–888
49. Mochizuki Y, Park MK, Mori T et al (1995) The difference in autofluorescence features of lipofuscin between brain and adrenal. Zool Sci 12:283–288
50. Croce AC, Bottiroli G (2014) Autofluorescence spectroscopy and imaging: a tool for biomedical research and diagnosis. Eur J Histochem 58:2461
51. Rózanowska M, Pawlak A, Rózanowski B et al (2004) Age-related changes in the photoreactivity of retinal lipofuscin granules: role of chloroform-insoluble components. Invest Ophthalmol Vis Sci 45:1052–1060
52. Otsuki J, Nagai Y, Matsuyama Y et al (2012) The influence of the redox state of follicular fluid albumin on the viability of aspirated human oocytes. Syst Biol Reprod Med 58:149–153
53. Otsuki J, Nagai Y, Chiba K (2007) Lipofuscin bodies in human oocytes as an indicator of oocyte quality. J Assist Reprod Genet 24:263–270
54. Siakotos AN, Watanabe I, Pennington K et al (1973) Procedures for the mass isolation of pure lipofuscins from normal human heart and liver. Biochem Med 7:25–38
55. Chang J, Wang Y, Shao L et al (2016) Clearance of senescent cells by ABT263 rejuvenates aged hematopoietic stem cells in mice. Nat Med 22:78–83
56. Sheehy MRJ (2008) Questioning the use of biochemical extraction to measure lipofuscin for age determination of crabs: comment on Ju et al. (1999, 2001). Mar Ecol Prog Ser 353:303–306
57. Crowley CE, Gandy RL, Daly KL et al (2014) Problems associated with a lipofuscin extraction method used to age blue crabs Callinectes sapidus cultured in Florida, USA. Aquat Biol 21:85–92
58. Manjunath S, Bola Sadashiva SR, Satyamoorthy K, et al (2014) Nature of autofluorescence in human serum albumin under its native, unfolding and digested forms. Proc SPIE 8935, advanced biomedical and clinical diagnostic systems. XII, 8935:893520
59. Wolfbeis SO, Leiner M (1985) Mapping of the total fluorescence of human blood serum as a new method for its characterization. Anal Chim Acta 167:203–215
60. Hegedus ZL, Altschule MD, Frank HA et al (1985) Increase in plasma lipofuscin levels of stored blood. Crit Care Med 13:155–159
61. Cequier-Sánchez E, Rodríguez C, Ravelo AG et al (2008) Dichloromethane as a solvent for lipid extraction and assessment of lipid classes and fatty acids from samples of different natures. J Agric Food Chem 56:4297–4303